Lab 3 Report
Vehicle vibration control by using PD, PID, Skyhook and $H\infty$ controllers

SD2231– Applied vehicle dynamics control

May 22, 2020

Anirvan Dutta
Akash Singh

Postal address
Royal Institute of Technology
KTH Vehicle Dynamics
SE-100 44 Stockholm
Sweden

Visiting address
Teknikringen 8
Stockholm

Telephone
+46 8 790 6000
Telefax
+46 8 790 9304

Internet
www.ave.kth.se

Contents

1 1DOF : Damped Passive System

1.1 Task 1.1

Natural frequency, ω_n is given by

$$\omega_n = \sqrt{\frac{k_p}{m_p}}[\frac{rad}{s}] \tag{1}$$

,where k_p is the spring stiffness and m_p the mass. Physically it signifies the frequency of the input at which the system produces maximum amplification and might go into unstable or sustained oscillations.

The damping ratio, ζ is given by

$$\zeta = \frac{c_p}{c_c} = \frac{c_p}{2\sqrt{k_p m_p}} \tag{2}$$

,where c_p is the damper coefficient, c_c is the critical damper coefficient. The damping ratio gives an idea about the oscillations in the output in case there is any change in the input.
Based on the value of ζ the system can be classified into under-damped, critically damped or over-damped. Comparing their responses to an impulse input,

- Under-damped systems with $0 < \zeta < 1$ has an extended oscillatory behavior before the output settles at a steady state.
- The critically damped system, with $\zeta = 1$, there is no oscillations observed.
- Similarly, the over-damped system, with $\zeta > 1$, also shows no oscillations but takes longer to reach the steady state.

1.2 Task 1.2

For the given system,
$m_p = 0.16kg$
$c_p = 0.4Ns/m$
$k_p = 6.32N/m$

So, the ω_n and ζ for the system are calculated as :

$$\omega_n = \sqrt{\frac{k_p}{m_p}} = 6.28rad/s$$
$$\zeta = \frac{c_p}{2\sqrt{k_p m_p}} = 0.4$$

1.3 Task 1.3

The transfer function for the base disturbance $z_w(s)$ to the displacement $z_p(s)$ of the mass is given by:

$$\begin{aligned}\frac{z_p(s)}{z_w(s)} &= \frac{c_p s + k_p}{m_p s^2 + c_p s + k_p} \\ &= \frac{2\zeta\omega_n s + {\omega_n}^2}{s^2 + 2\zeta\omega_n s + {\omega_n}^2}\end{aligned} \tag{3}$$

The figure 1 shows the bode plot of the transfer function comparing the given system with that where $c_p = 0$, i.e an undamped system.

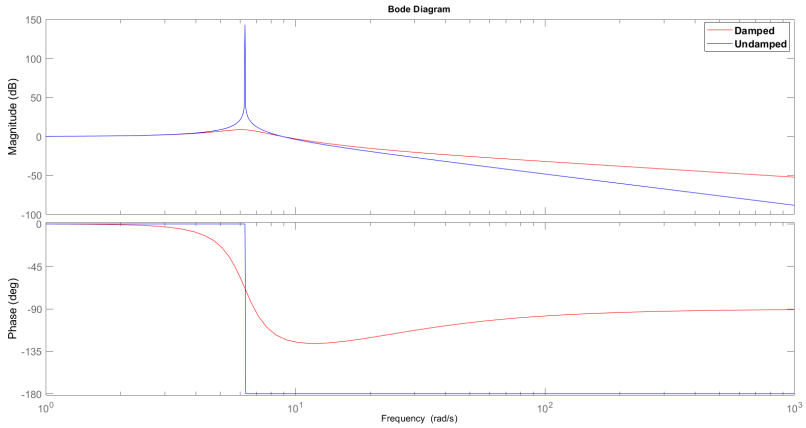

Figure 1: Bode plot for given c_p and $c_p = 0$

From the bode plot also, the ω_n is found to be $6.28 rad/s$.

1.4 Task 1.4

The figure 2 shows the impulse and step response of the 3 different systems.

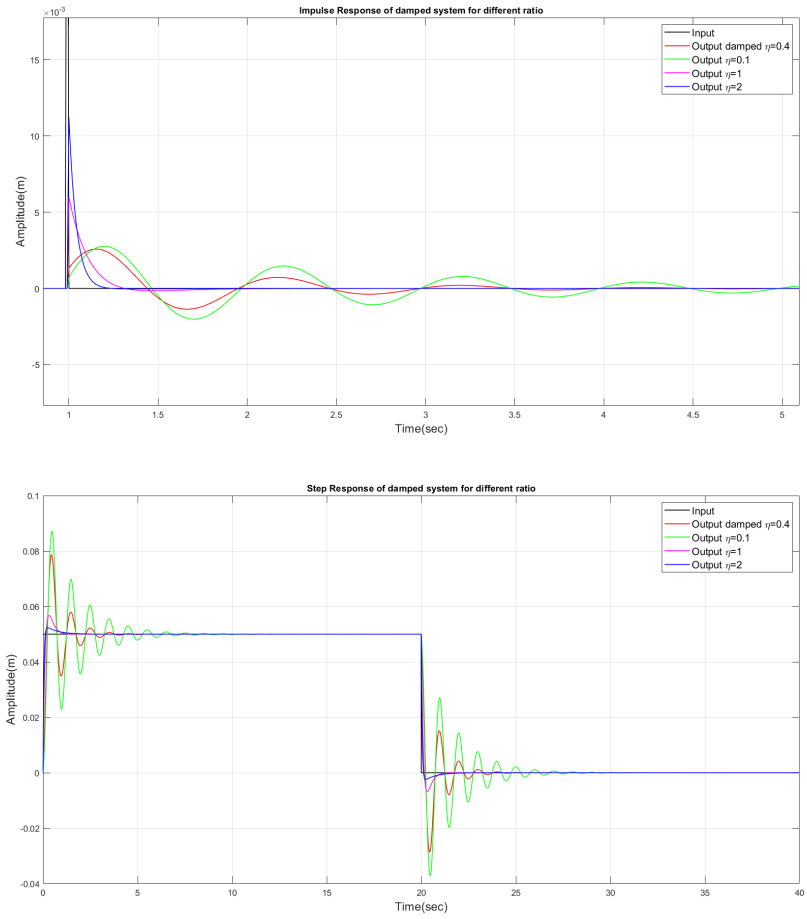

Figure 2: Impulse and step response of systems with different damping ratios

[1] As can be seen in the figure 2, the $\zeta = 1$ does not lead to no oscillations in the output, since the transfer function contains a zero. The definition given in task 1.1 applies to the collocated systems where the force is applied on the same mass whose displacement is being observed. But still, the given system also follows the trend of decreasing oscillations with increasing magnitude of damping ratio ζ.

[1] We have considered impulse excitation as a signal that exists for only one time step. But we have also included step input, which conforms with the mathematical definition of the excitation provided in the hand-out.

2 1DOF : Active Control-PD

2.1 Task 2.1

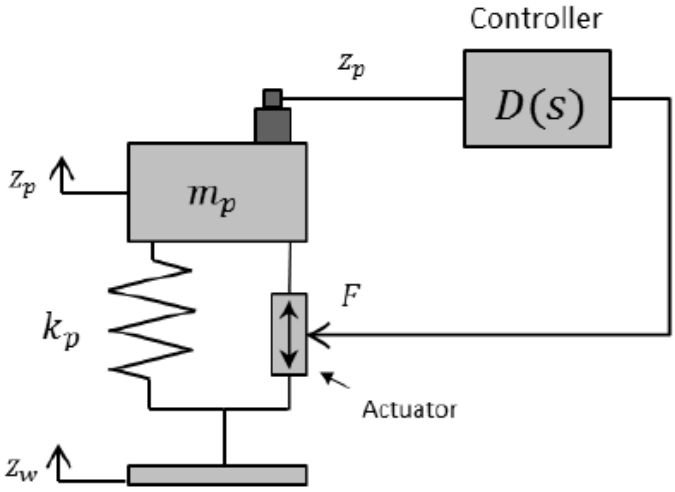

Figure 3: Mass Spring system with an active PD controlled damper

The equations of motion for the system in figure 3 are given as :

$$m_p \frac{d^2 z_p(t)}{dt^2} = -k_p(z_p(t) - z_w(t)) + F(t) \tag{4}$$

$$F(t) = -d_p z_p(t) - d_d \dot{z}_p(t) \tag{5}$$

Once we convert these equations of motion into laplace domain, we get the transfer function for $\frac{z_p(s)}{z_w(s)}$

$$\frac{z_p(s)}{z_w(s)} = \frac{k_p}{m_p s^2 + d_d s + (k_p + d_p)} \tag{6}$$

2.2 Task 2.2

Comparing the denominator of transfer function, given in 6 with that of the passive system's tranfer function, i.e $m_p s^2 + c_p s + k_p$, we get the intial estimates for d_p and d_d.
$d_d \approx c_p$
$d_p \approx 0$

2.3 Task 2.3

In order to tune the parameters, d_p and d_d, we performed a 2-D grid search, where we let the algorithm find the best fit parameters in the neighborhood of our initial estimates. We considered :

- Overshoot reduction : Comparing of the magnitude of sinusoidal and impulse response magnitude.

- Ensuring oscillation : Determining the peaks of impulse response and ensuring is under critically damped response.
- Ensuring faster damping : Comparing the steady state time of impulse response.

We found the final values for them do be $d_d = 1.2$ and $d_p = 0.01$. P.S : We kept the value of d_p to be close to zero in order to not affect the natural frequency of the system. Figure 4 shows the difference in performance of tuned vs untuned PD controller.

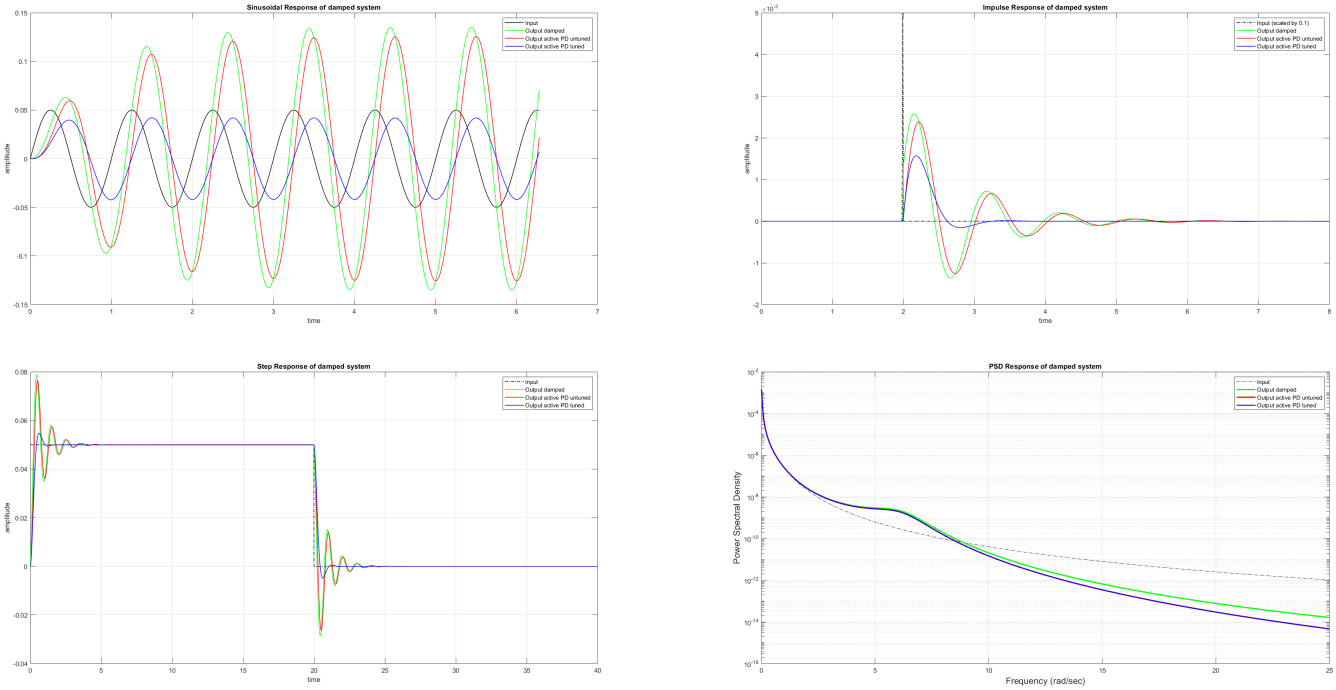

Figure 4: Difference between performance of the PD Controller for tuned and untuned parameters

3 1DOF : Active Controller-PID

3.1 Task 3.1

Similar to the previous case of PD controller, the equations of motion are given as :

$$m_p \frac{d^2 z_p(t)}{dt^2} = -k_p(z_p(t) - z_w(t)) + F(t) \tag{7}$$

$$F(t) = -h_p z_p(t) - h_d \dot{z}_p(t) - h_i \int_0^t z_p(t)dt \tag{8}$$

Subsequently, the transfer function is derived as follows

$$\frac{z_p(s)}{z_w(s)} = \frac{k_p s}{m_p s^3 + h_d s^2 + (k_p + h_p)s + h_i} \tag{9}$$

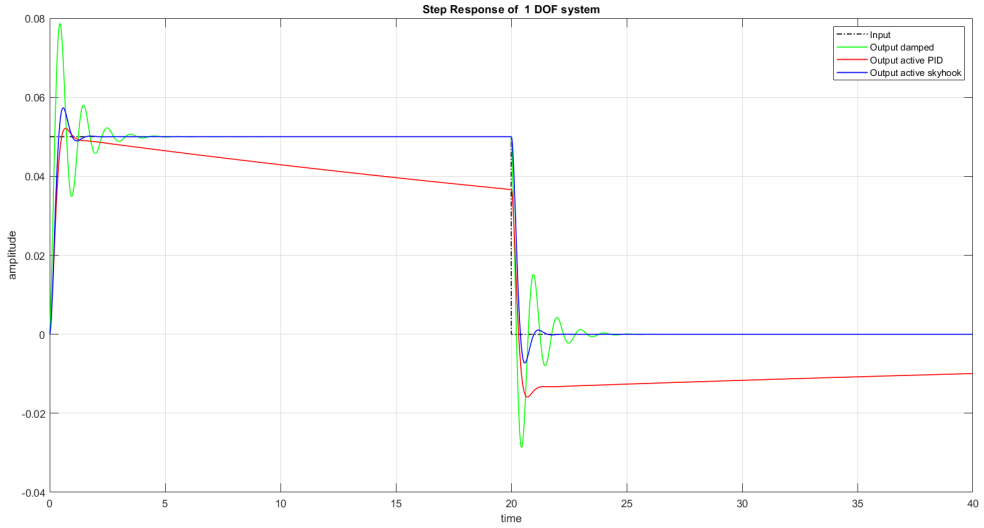

Figure 5: Problematic step response with PID-controlled damper

The PID parameters, h_p, h_d h_i, were found in a similar manner as with PD controller, using the grid search The final value of tuned parameters was found to be: $h_p = 0.01$, $h_d = 1.4$, $h_i = 0.1$ Keeping a higher value of h_i helps in reducing oscillations and lowering noise amplification of the system, but we see the problem with high value of h_i in case a step input is given to the system. Due to inherent nature of integral controller, it always tries to drive the output towards zero, so the system will not stabilise at the desired steady state, as is shown in figure 5.

Physically, it would mean that even if the road elevation changes, the suspension system would slowly go back to its zero steady state position. Thus, reducing ground clearance of the vehicle.

The remaining responses of the system towards different excitations are provided in the figure 6 in the next section aling with the results of the skyhook controller, for a better comparison.

4 1DOF : Active Controller-Skyhook

4.1 Task 4.1

The equations of motion and the transfer function for system employing a skyhook controller are very similar to that of the one using PD controller, with $d_p = 0$.

Transfer function $\frac{z_p(s)}{z_w(s)}$ is given by :

$$\frac{z_p(s)}{z_w(s)} = \frac{k_p}{m_p s^2 + d_d s + k_p} \tag{10}$$

The figure 6 provides easy comparison between performance of skyhook and PID controller.

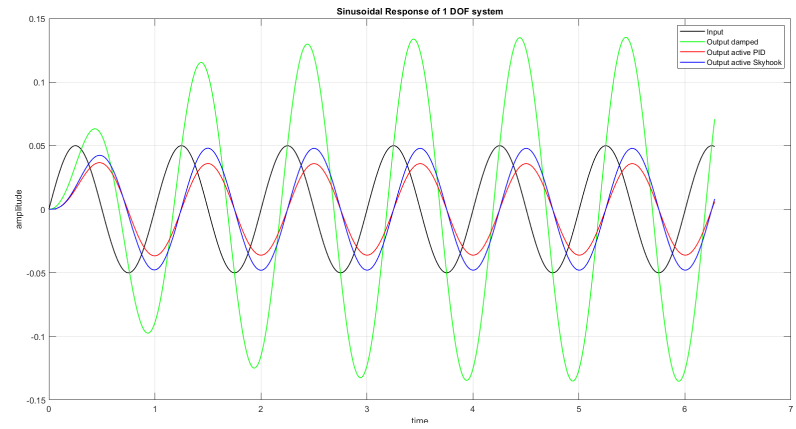

(a)

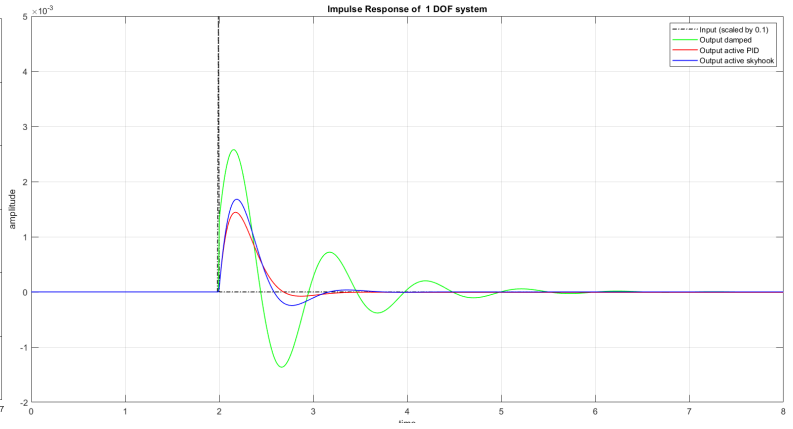

(b)

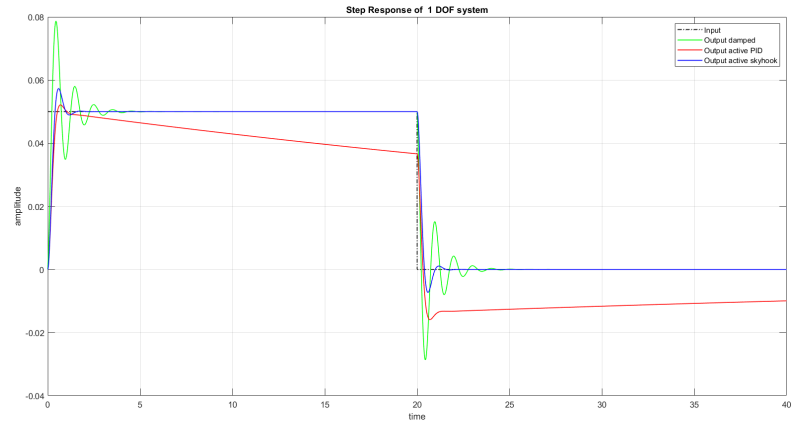

(c)

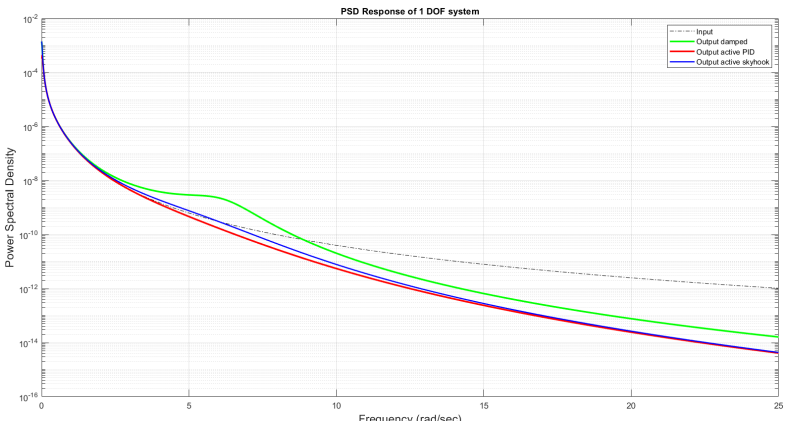

(d)

Figure 6: System Responses for different excitations for PID and Skyhook controller

5 1DOF : Summary

5.1 Task 5.1

The figure 7 shows that all the active controllers have a lower amplitude of the transfer function as compared to the passively damped system.

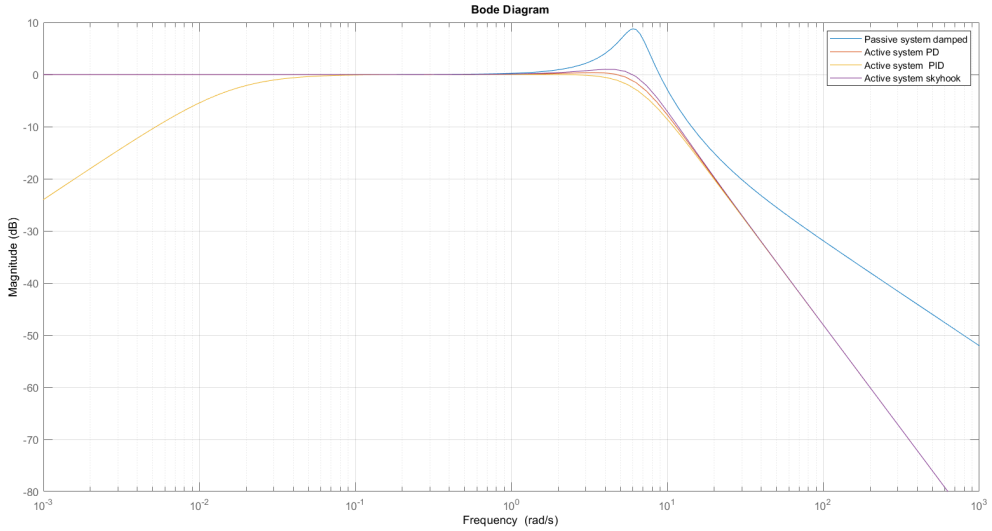

Figure 7: Comparing amplitude of all the transfer functions

5.2 Task 5.2

A summary of controller performances is repeated here in figure 8.

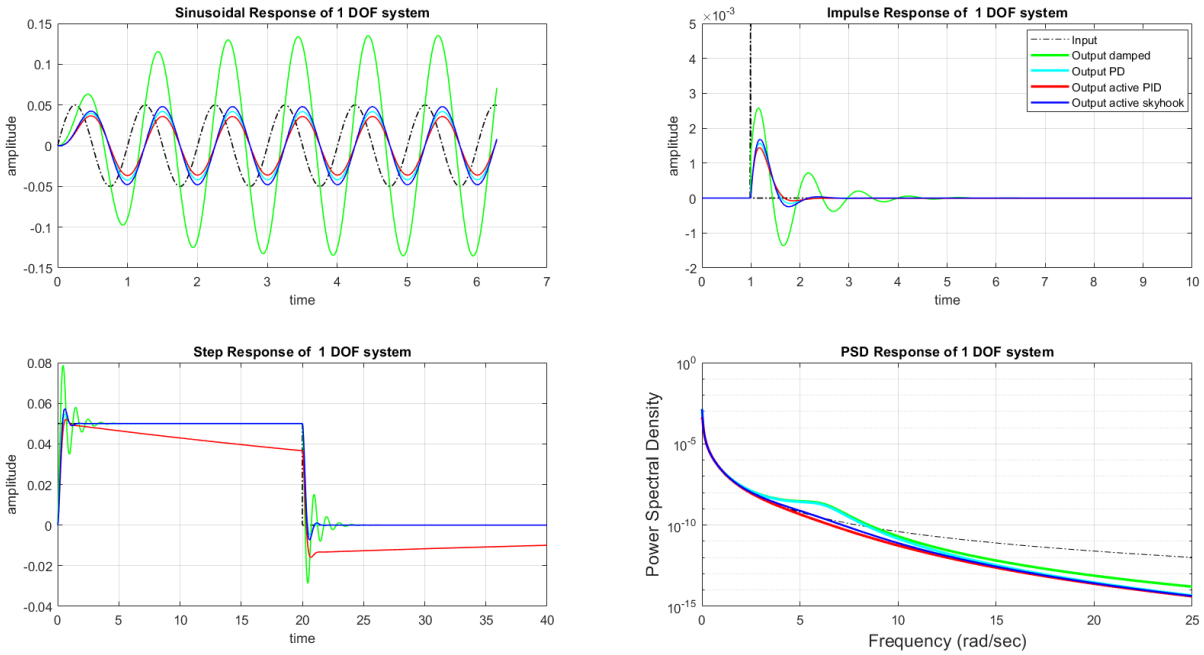

Figure 8: Comparing responses to different base excitations

6 2DOF : Damped Passive System

6.1 Task 6.1

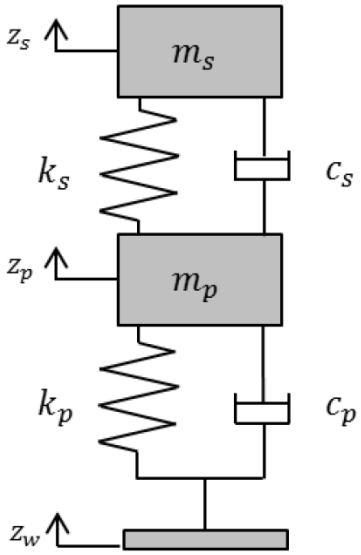

Figure 9: 2 DOF coupled mass system

The equations of motion for the system in figure 9 are given as :

$$\begin{aligned} m_s\frac{d^2z_s(t)}{dt^2} &= -k_p(z_s(t)-z_p(t)) - C_s(\dot{z}_s-\dot{z}_p) \\ m_p\frac{d^2z_p(t)}{dt^2} &= -k_p(z_p(t)-z_w(t)) - k_p(z_s(t)-z_p(t)) - C_s(\dot{z}_s-\dot{z}_p) - C_p(\dot{z}_p-\dot{z}_w) \end{aligned} \tag{11}$$

Once we convert these equations of motion into laplace domain, after rearranging the terms, we get the transfer function for $\frac{z_s(s)}{z_w(s)}$

$$\frac{z_s(s)}{z_w(s)} = \frac{c_pc_ss^2 + (c_pk_s + c_sk_p)s + k_pk_s}{m_pm_ss^4 + (m_sc_p + m_sc_s + m_pc_s)s^3 + (m_sk_p + m_sk_s + m_pk_s + c_pc_s)s + (c_sk_p + c_pk_s)s + k_pk_s}$$

6.2 Task 6.2

The figure 10 clearly shows the advantage of having 2 level of suspensions. As can be seen the magnitude of the transfer function at high frequencies is much less now, leading to the system being lesser affected by the noise at the base.

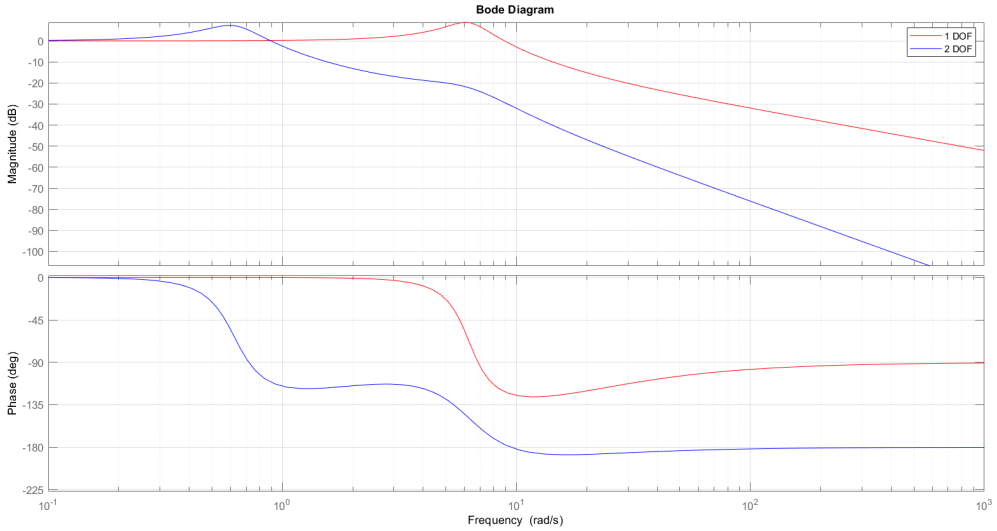

Figure 10: Bode plot 2 DOF vs 1 DOF passive system

The response to excitations is shown along with the results of Task 7.1.

2DOF : Active Controller-Skyhook

6.3 Task 6.3

The state space representation of the system is also derived from the equations of motion. The equations are very similar to equations 11, where the damper force is replaced by actuator force $F(t)$, which is given by

$$F(t) = -T\dot{z}_s \tag{12}$$

The state space representation for the skyhook controlled system is given by eq 13

$$x = \begin{bmatrix} z_s & \dot{z}_s & z_p & \dot{z}_p \end{bmatrix}^T$$

$$U = \begin{bmatrix} z_w & \dot{z}_w \end{bmatrix}^T$$

$$A_{sk} = \begin{bmatrix} 0 & 1 & 0 & 0 \\ -\frac{k_s}{m_s} & -\frac{T}{m_s} & \frac{k_s}{m_s} & 0 \\ 0 & 0 & 0 & 1 \\ \frac{k_s}{m_p} & \frac{T}{m_p} & -\frac{k_s+k_p}{m_s} & -\frac{c_p}{m_p} \end{bmatrix}$$

$$B_{sk} = \begin{bmatrix} 0 & 0 \\ 0 & 0 \\ 0 & 0 \\ \frac{k_p}{m_p} & \frac{c_p}{m_p} \end{bmatrix}$$

$$C_{sk} = \begin{bmatrix} 1 & 0 & 0 & 0 \end{bmatrix}$$

$$D_{sk} = \begin{bmatrix} 0 & 0 \end{bmatrix} \tag{13}$$

6.4 Task 6.4

The implementation of skyhook controller using state space representation given by eq 13 in simulink is shown in figure 11.

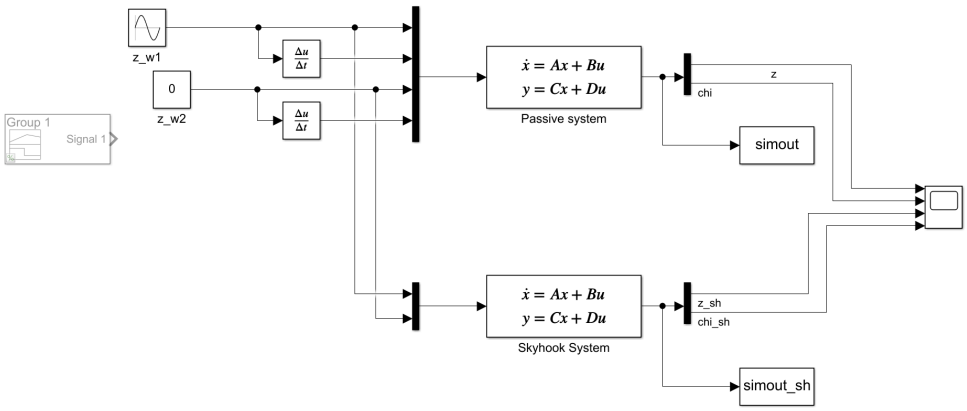

Figure 11: Simulink setup of 2 DOF system

7 2DOF : Summary

7.1 Task 7.1

A summary of the results for passively damped system and active skyhook controlled damper is presented in figure 12. The Skyhook controller works better than the damped passive system, and also satisfies all the requirements mentioned in the handout. Also, as we can see in figure 12, the value of $T = 1$

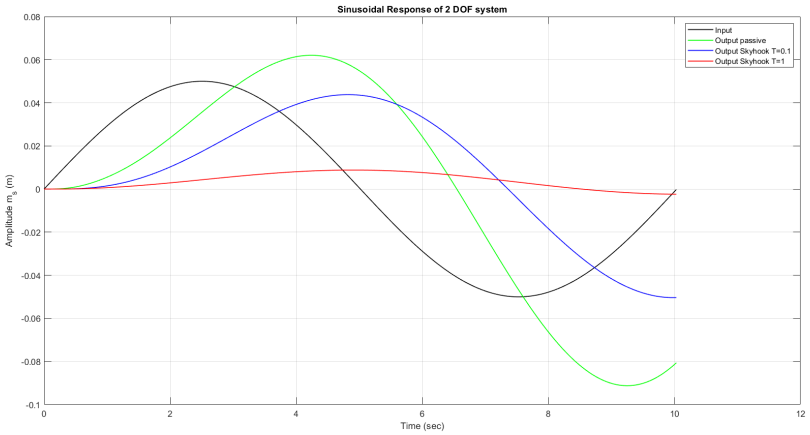

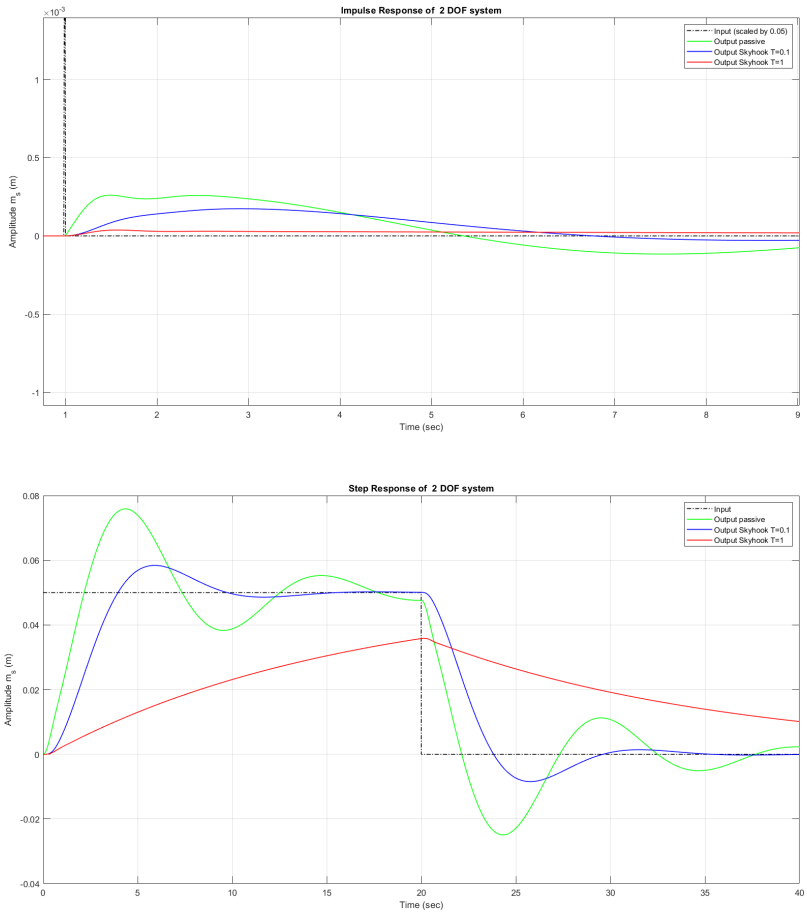

Figure 12: Response of 2 DOF passive and skyhook system with different damping ratios

leads to an over damped system, which is also not desirable. So the margin of tuning T here is very narrow.

8 Control of bounce and pitch for a simple vehicle model using Sky-hook and H_∞

8.1 Task 8.1

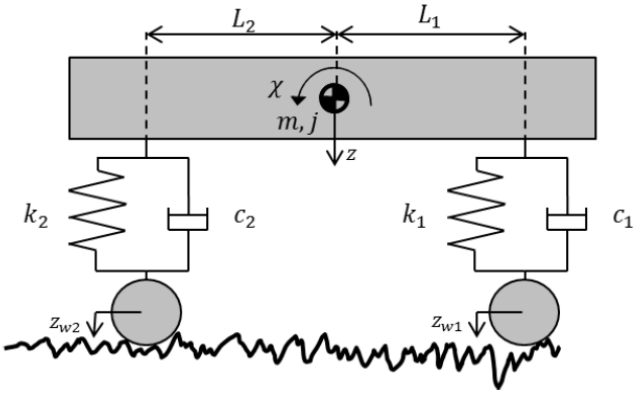

Figure 13: Vehicle model with passive suspension

The bounce and pitch equations of motion for the vehicle model shown in figure.13 was derived as follows using the rail dynamics reference.

$$m\ddot{z} = -(k_1+k_2)z-(c_1+c_2)\dot{z}+(k_1l_1-k_2l_2)\chi+(c_1l_1-c_2l_2)\dot{\chi} \quad (14)$$
$$+k_1z_{w1}+c_1\dot{z}_{w1}+k_2z_{w2}+c_2\dot{z}_{w2}$$
$$J\ddot{\chi} = (k_1l_1-k_2l_2)z+(c_1l_1-c_2l_2)\dot{z}-(k_1l_1^2+k_2l_2^2)\chi-(c_1l_1^2+c_2l_2^2)\dot{\chi} \quad (15)$$
$$-k_1l_1z_{w1}-c_1l_1\dot{z}_{w1}+k_2l_2z_{w2}+c_2l_2\dot{z}_{w2}$$

The state space representation of the equations in 14 is derived as follows considering the state $X = [z, \dot{z}, \chi, \dot{\chi}]^T$ and input as $u = [z_{w1}, \dot{z}_{w1}, z_{w2}, \dot{z}_{w2}]^T$

$$A = \begin{bmatrix} 0 & 1 & 0 & 0 \\ \frac{-(k_1+k_2)}{m} & \frac{-(c_1+c_2)}{m} & \frac{(k_1l_1-k_2l_2)}{m} & \frac{(c_1l_1-c_2l_2)}{m} \\ 0 & 0 & 0 & 1 \\ \frac{(k_1l_1-k_2l_2)}{J} & \frac{(c_1l_1-c_2l_2)}{J} & \frac{-(k_1l_1^2+k_2l_2^2)}{J} & \frac{-(c_1l_1^2+c_2l_2^2)}{J} \end{bmatrix} \quad (16)$$

$$B = \begin{bmatrix} 0 & 0 & 0 & 0 \\ \frac{k_1}{m} & \frac{c_1}{m} & \frac{k_2}{m} & \frac{c_2}{m} \\ 0 & 0 & 0 & 1 \\ \frac{-k_1l_1}{J} & \frac{-c_1l_1}{J} & \frac{k_2l_2^2}{J} & \frac{c_2l_2^2}{J} \end{bmatrix}$$

$$C = \begin{bmatrix} 0 & 1 & 0 & 0 \\ 0 & 0 & 0 & 1 \end{bmatrix} \quad D = zeros(2,4)$$

8.2 Task 8.2

The natural frequency of each dimension of bounce z and pitch χ can be found as

$$\omega_z = \sqrt{\frac{k_1+k_2}{m}} = 7.38 rad/s \;\; \omega_\chi = \sqrt{\frac{k_1 l_1^2 + k_2 l_2^2}{J}} = 7.86 rad/s \tag{17}$$

This was also verified using the MATLAB's `damp` function. The responses of the passive system were generated for the different excitation and are shown with the Skyhook and H_∞ controllers in the next section.

9 Vehicle Model : Skyhook

9.1 Task 9.1

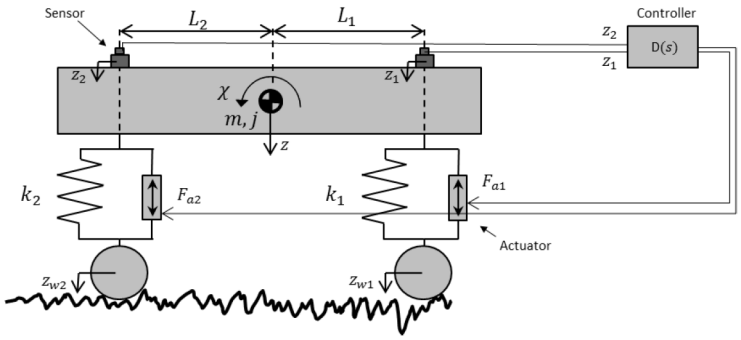

Figure 14: Vehicle model with active suspension

The bounce and pitch equations of motion for the vehicle model shown in figure.14 was derived as follows using the rail dynamics reference.

$$\begin{aligned} m\ddot{z} &= -(k_1+k_2)z + (k_1 l_1 - k_2 l_2)\chi + k_1 z_{w1} + k_2 z_{w2} - F_{a1} - F_{a2} \\ J\ddot{\chi} &= (k_1 l_1 - k_2 l_2)z - (k_1 l_1^2 + k_2 l_2^2)\chi - -k_1 l_1 z_{w1} + k_2 l_2 z_{w2} + F_{a1} l_1 - F_{a2} l_2 \end{aligned} \tag{18}$$

The state space representation of the equations in 18 is derived as follows considering the state $X = [z, \dot{z}, \chi, \dot{\chi}]^T$ and input as $u = [z_{w1}, z_{w2}, F_{a1}, F_{a2}]^T$

$$A = \begin{bmatrix} 0 & 1 & 0 & 0 \\ \frac{-(k_1+k_2)}{m} & 0 & \frac{(k_1 l_1 - k_2 l_2)}{m} & 0 \\ 0 & 0 & 0 & 1 \\ \frac{(k_1 l_1 - k_2 l_2)}{J} & 0 & \frac{-(k_1 l_1^2 + k_2 l_2^2)}{J} & 0 \end{bmatrix} \tag{19}$$

$$B = \begin{bmatrix} 0 & 0 & 0 & 0 \\ \frac{k_1}{m} & \frac{k_2}{m} & \frac{-1}{m} & \frac{-1}{m} \\ 0 & 0 & 0 & 1 \\ \frac{-k_1 l_1}{J} & \frac{k_2 l_2^2}{J} & \frac{l_1}{J} & \frac{-l_2}{J} \end{bmatrix}$$

$$C = \begin{bmatrix} 0 & 1 & 0 & 0 \\ 0 & 0 & 0 & 1 \end{bmatrix} \quad D = zeros(2,4)$$

9.2 Task 9.2

The relation between F_z, T_χ and F_{a1},F_{a2} can be found from the force and torque balancing equations.

$$\begin{aligned} F_z(t) &= c_z\dot{z} = F_{a1} + F_{a2} \\ T_\chi(t) &= -c_\chi\dot{\chi} = F_{a1}L_1 - F_{a2}L_2 \end{aligned} \tag{20}$$

On solving the above equations, we get the expression for F_{a1} and F_{a2} as -

$$\begin{aligned} F_{a1} &= \frac{c_z l_2\dot{z} - c_\chi\dot{\chi}}{(l_1+l_2)} \\ F_{a1} &= \frac{c_z l_1\dot{z} + c_\chi\dot{\chi}}{(l_1+l_2)} \end{aligned} \tag{21}$$

9.3 Task 9.3

The values of $c_z = 1e5$ and $c_x = 3e6$ were found to satisfying all the requirements for a good response and also the actuator forces are well below 10kN, as can be seen in figure 15.

Choosing very high values for c_z & c_x might lead to unrealistically high actuators forces, which in reality would just saturate the actuator and affect the system performance and actuator life.

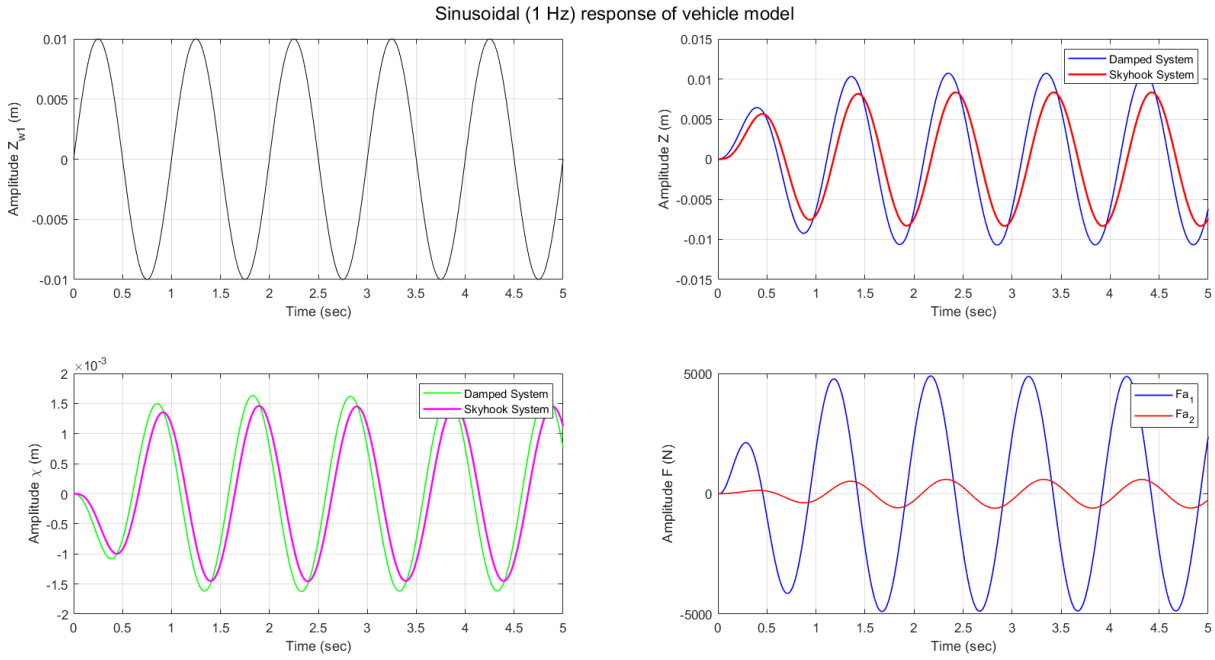

Sinusoidal (8 Hz) response of vehicle model

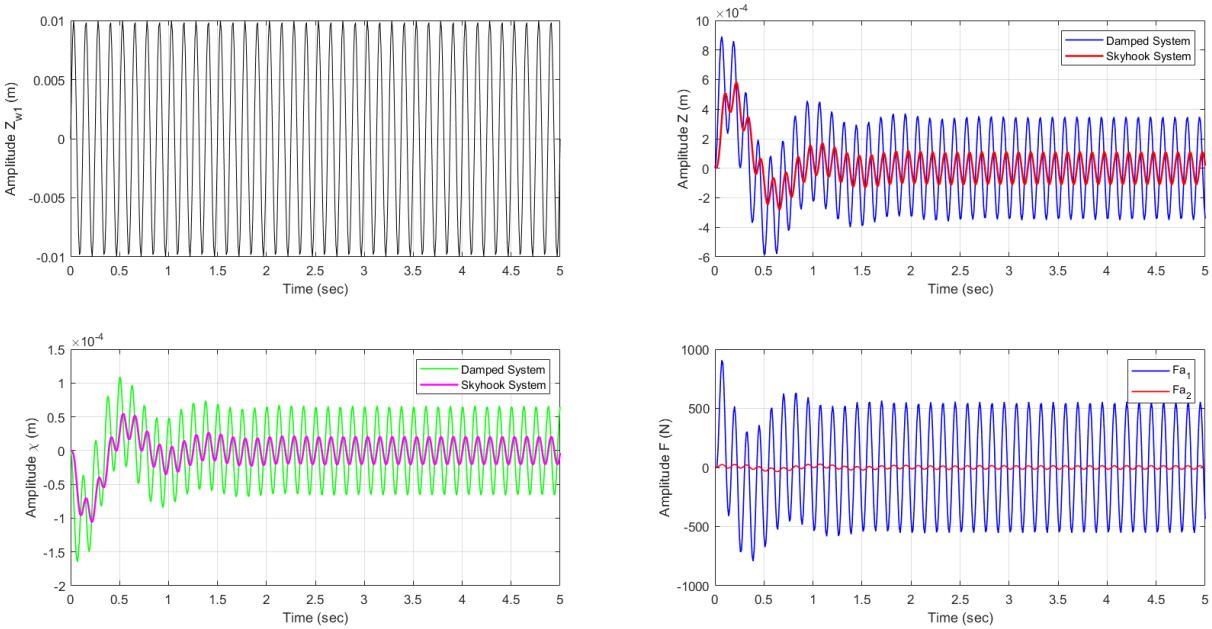

Impulse response of vehicle model

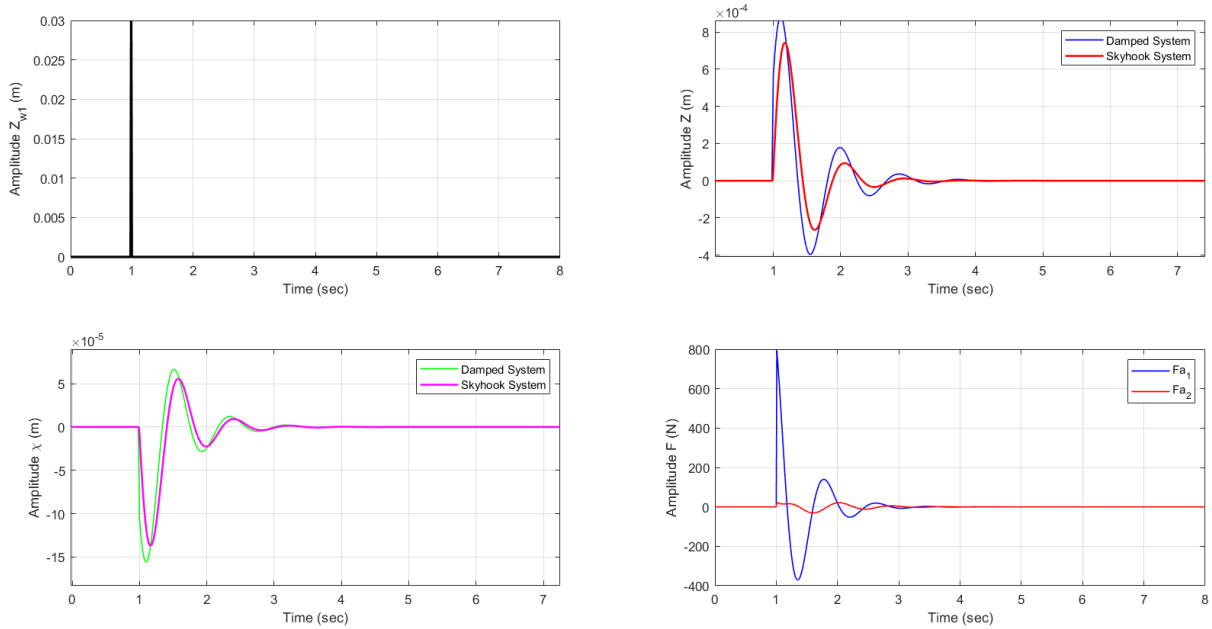

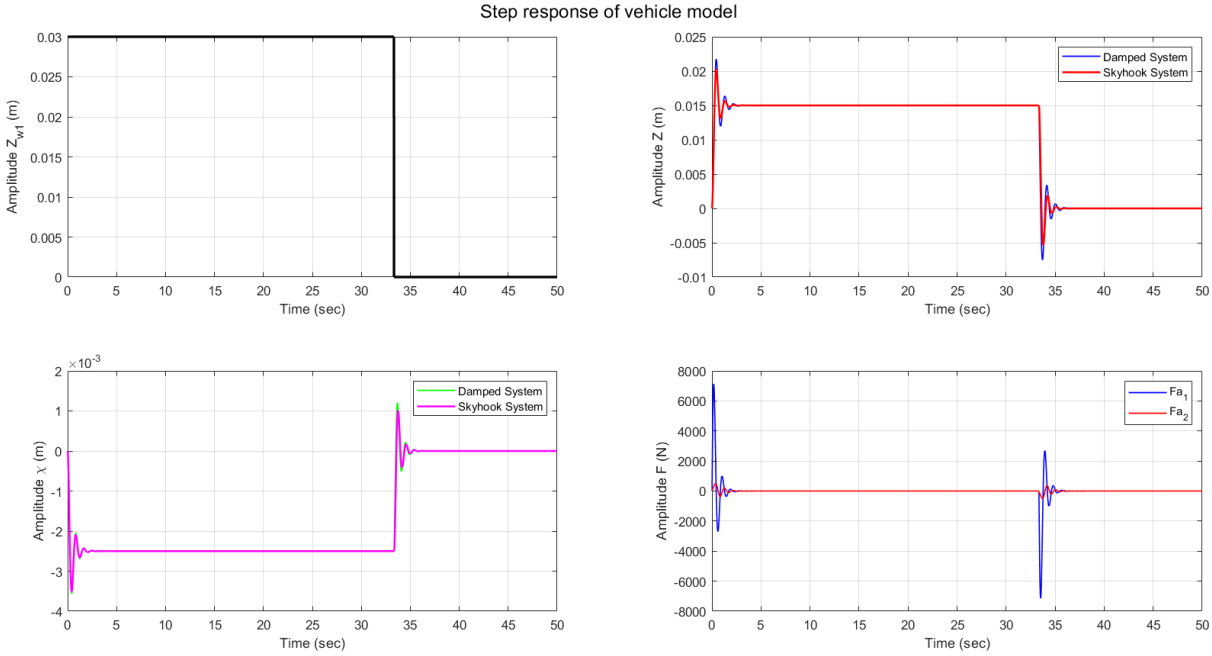

Figure 15: Response of vehicle passive and Skyhook system

10 Vehicle Model : H_∞ Controller

10.1 Task 10.1

Similar to Task 8.2, the natural frequency of the vehicle was obtained.

$$w_{nb} == \sqrt{\frac{k_1+k_2}{m}} = 7.38 rad/s \;\; w_{n\chi} = \sqrt{\frac{k_1 l_1^2 + k_2 l_2^2}{J}} = 7.86 rad/s \tag{22}$$

The system has the maximum gain at this frequency and should be penalized using the weighing functions. This was also by plotting the maximum singular value of the system as shown in figure.16

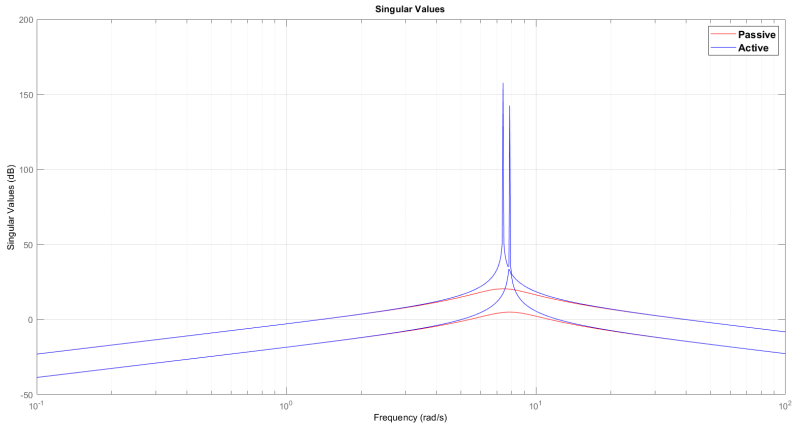

Figure 16: Singular values of the MIMO passive and active system

The gains of the W_b and W_χ were selected after iterative tuning based on response requirement of the H_∞ controller.

10.2 Task 10.2

The H_∞ controller was found using `hinfsys`, where $k_b = 2.055e3$ & $k_\chi = 4.1404e4$. The corresponding state space model of the controlled was implemented using Simulink as shown in figure 17.

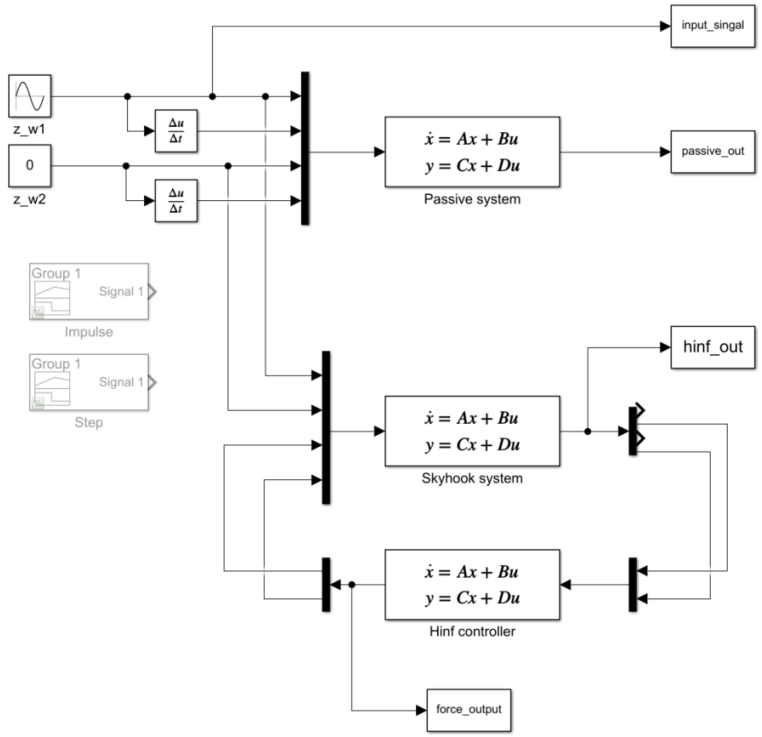

Figure 17: Simulink setup of vehicle system

The figure 18 shows the response of the system using H_{inf} controller to different excitations.

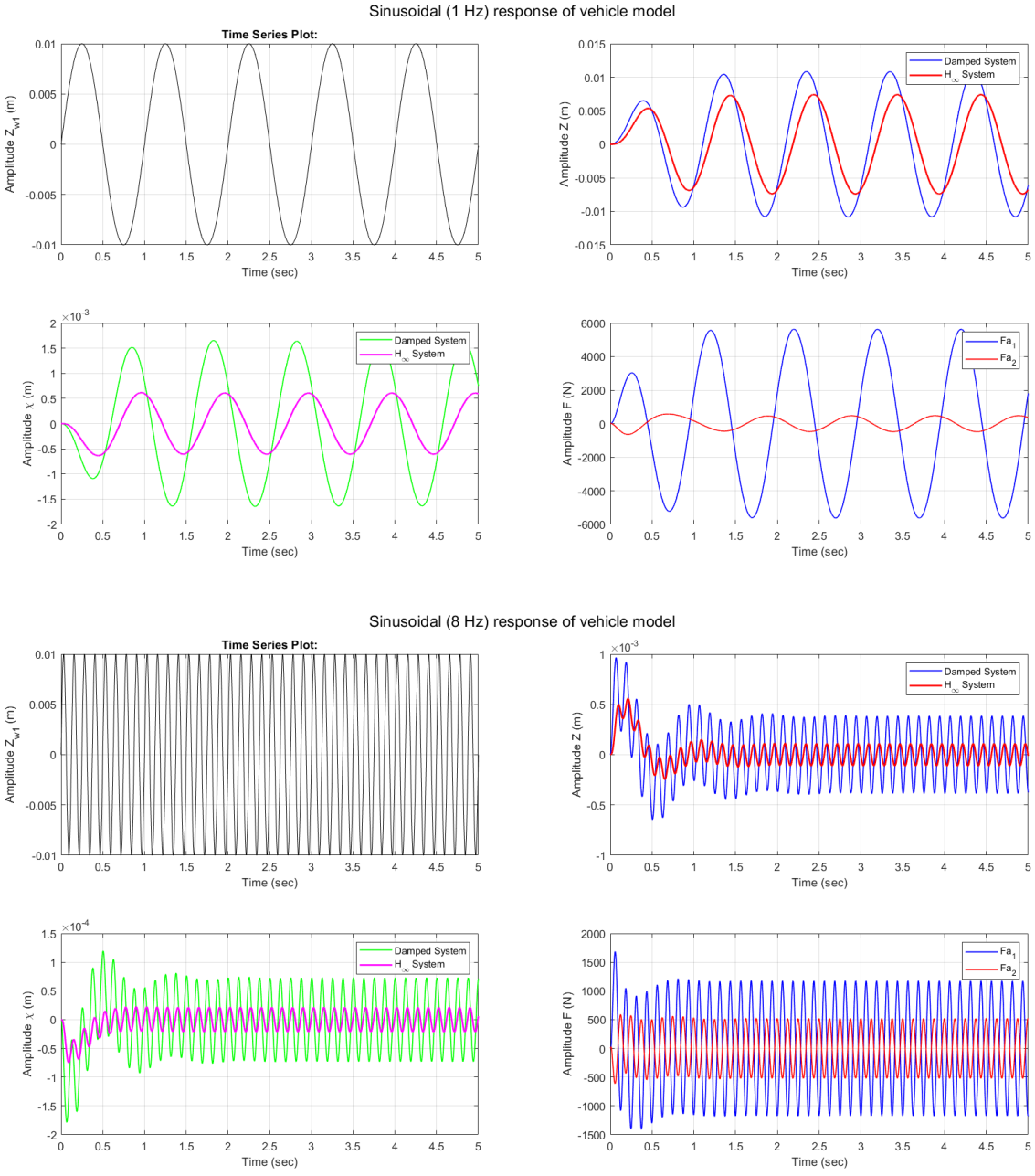

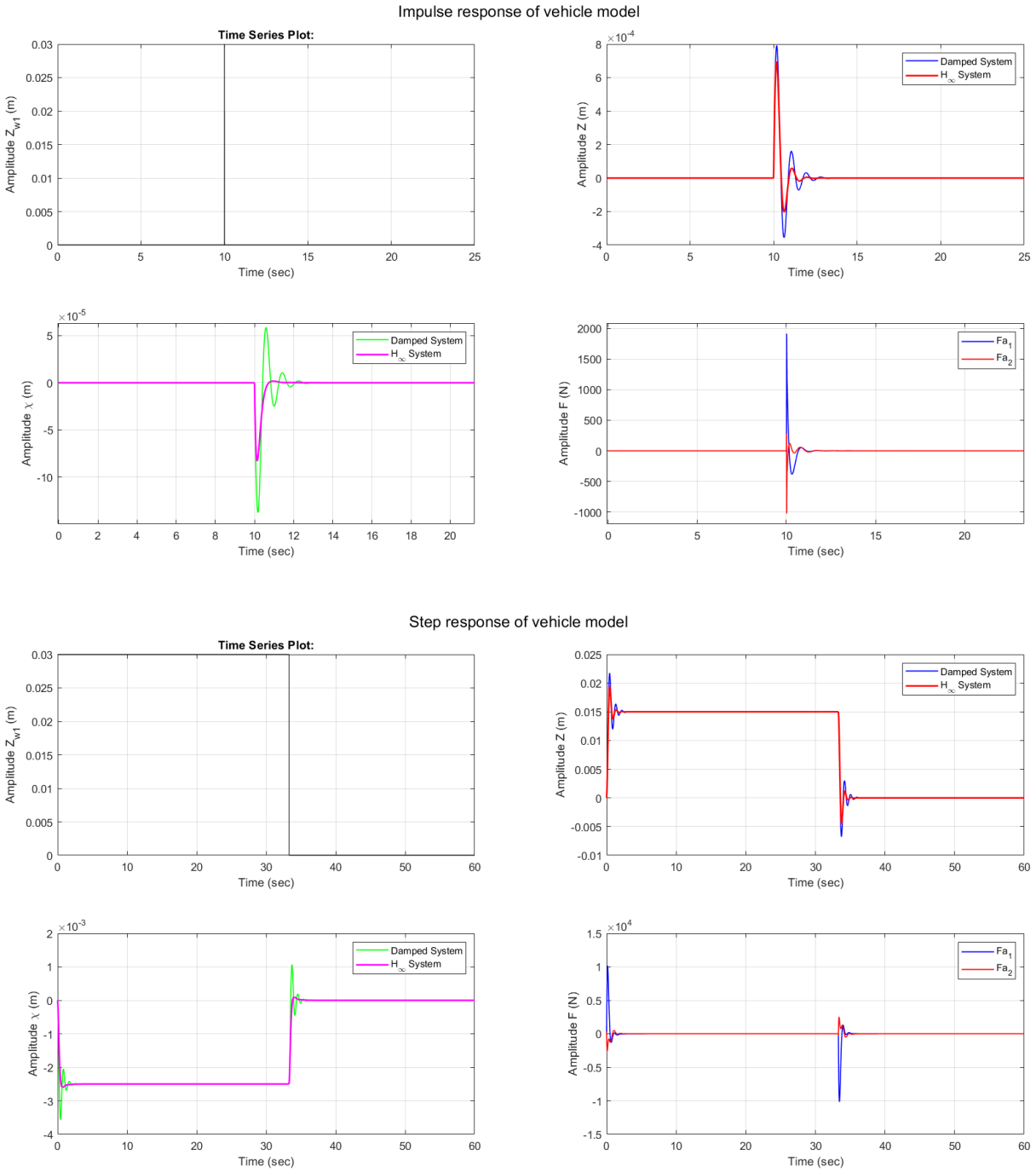

Figure 18: Response of vehicle passive and H_∞ controller

10.3 Task 10.3

The vehicle parameters mass, inertia and stiffness was varied within 15% tolerance to obtain the response of the both skyhook and H_∞ controller as shown in figure.19. Following observations were made -

- Since the H_∞ controller response was more damped than skyhook, the change in parameters effect was less pronounced in the H_∞ response
- The change in stiffness violated the constrain of force of 10 kN for the H_∞ response
- Skyhook controller was able to handle the uncertainty in all cases while satisfying the force constraint.
- Decreasing the mass and stiffness made the system induced longer settling time with mimimal increment in amplitude, thereby increasing stablity.

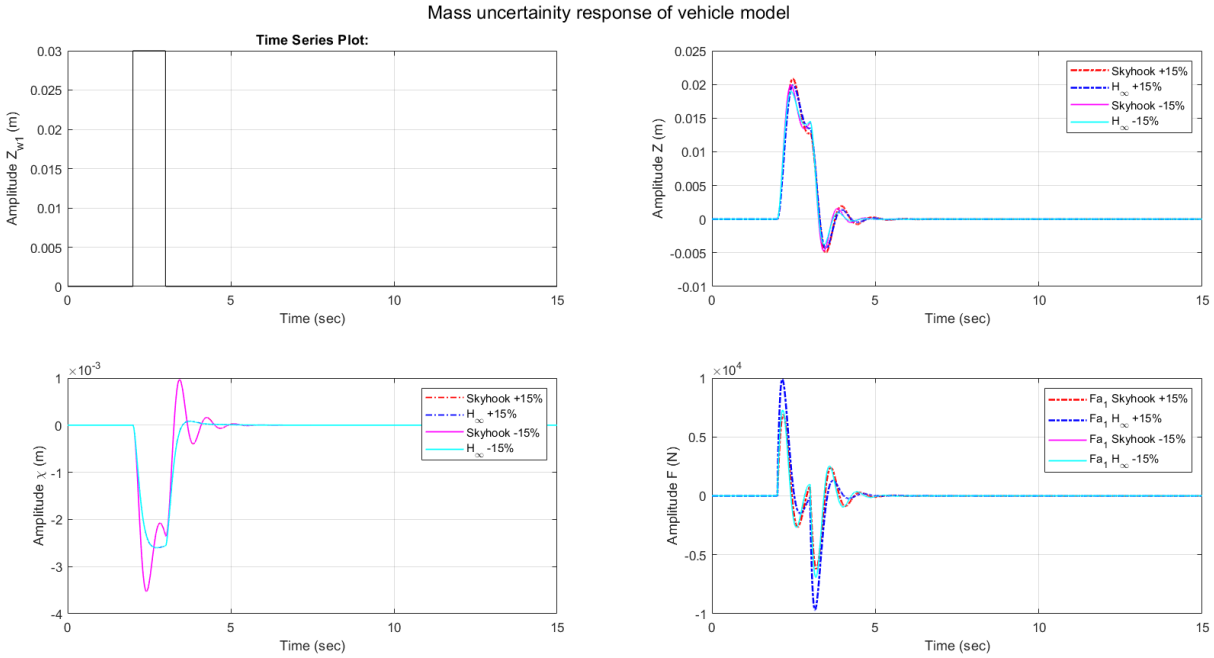

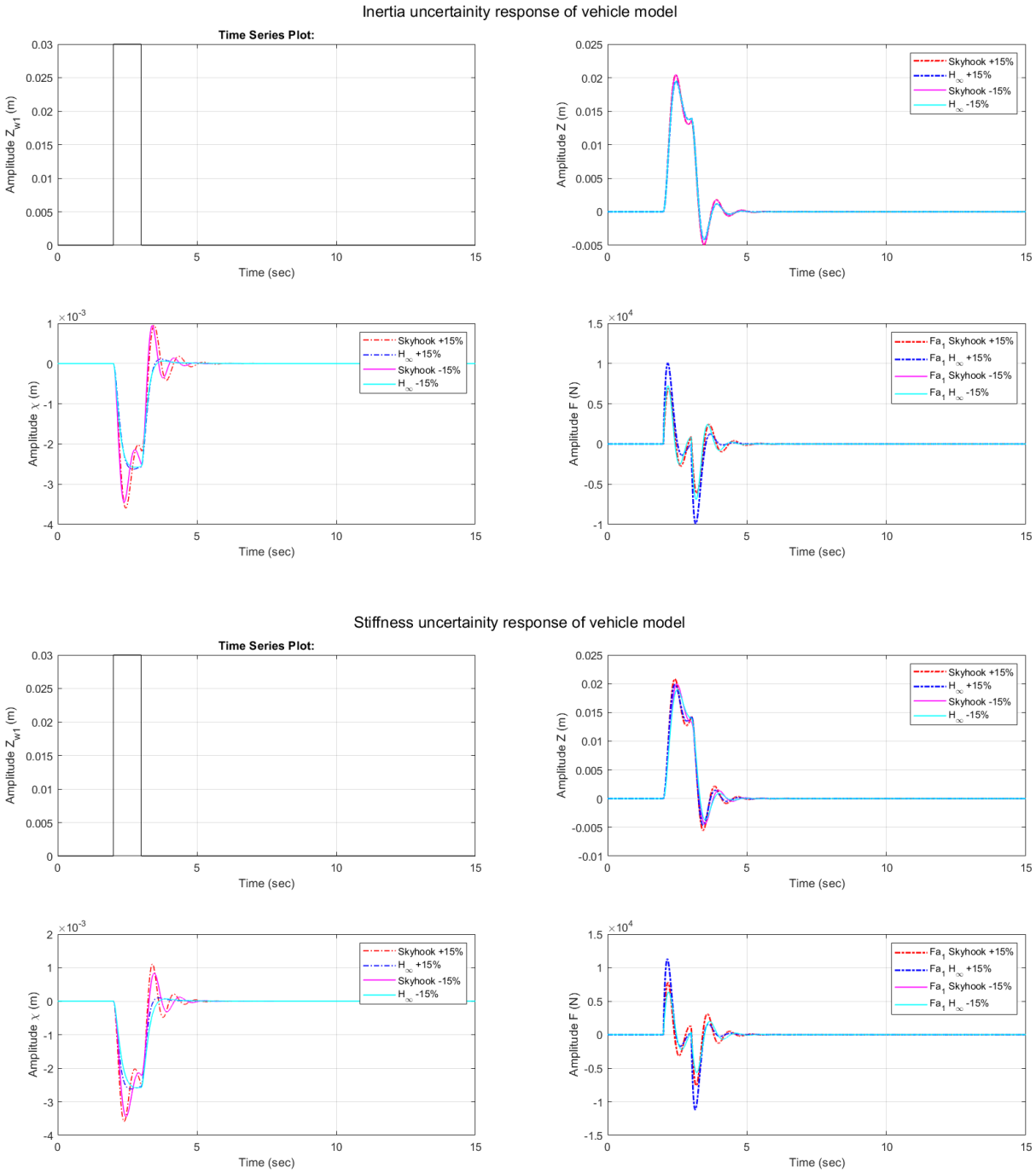

Figure 19: Response of vehicle controller for change in mass, inertia and stiffness

11 Vehicle Summary

11.1 Task 11.1

The response of the passive system, Skyhook and H_∞ to different excitations are presented in figure.20. The H_∞ performs better than Skyhook and is quite close to being critically damped on the expense of larger force values.

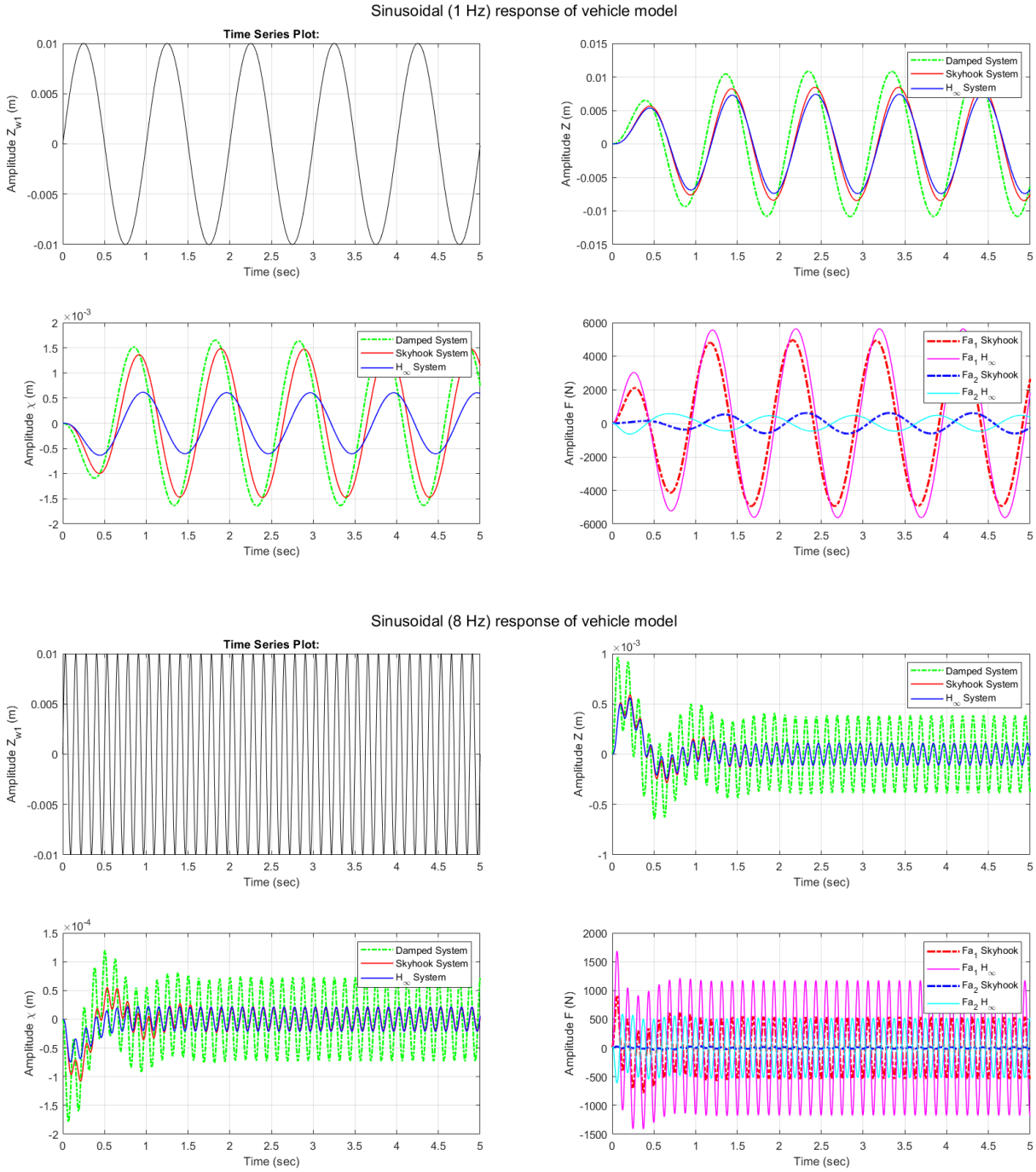

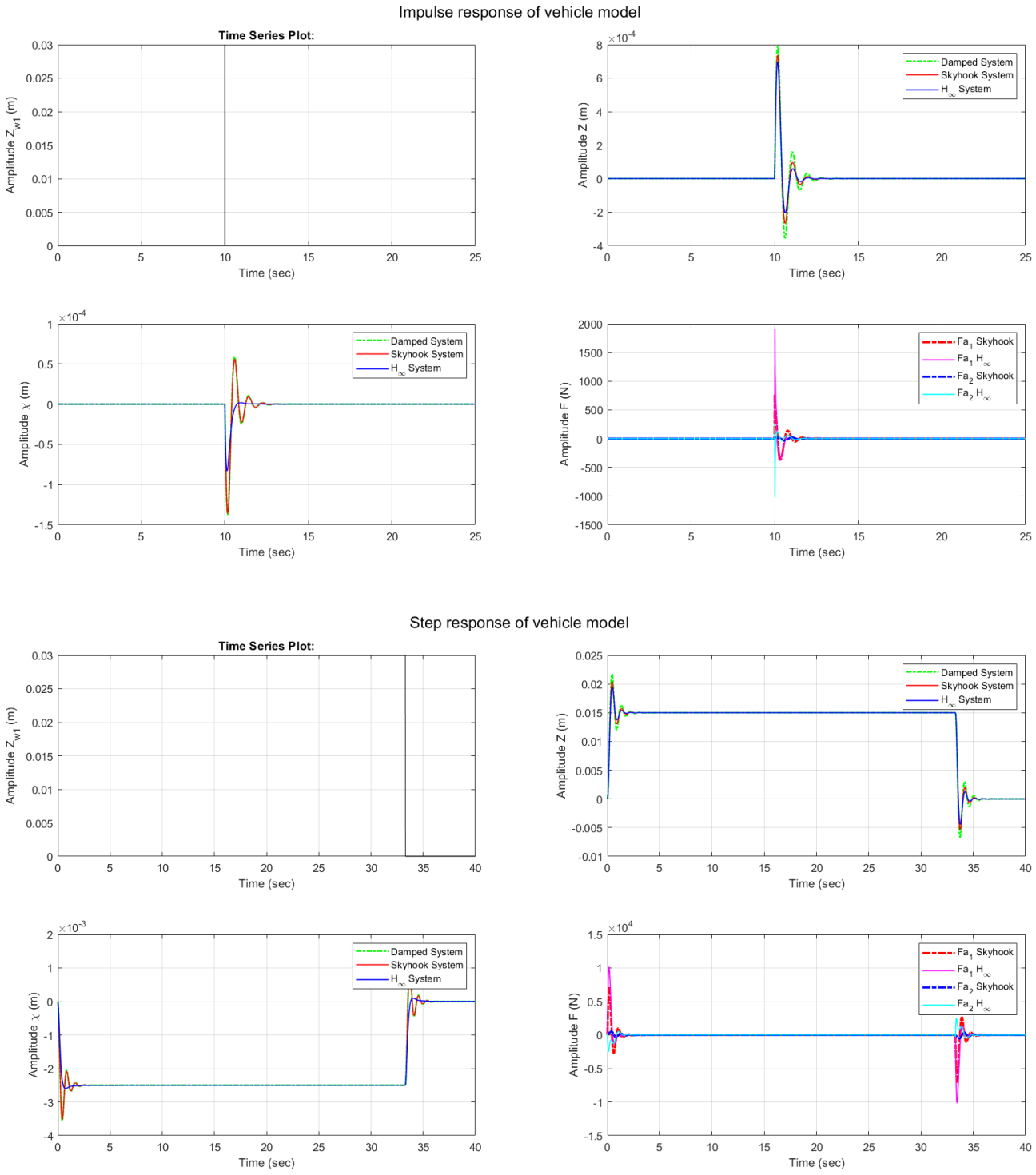

Figure 20: Response of vehicle passive, Skyhook H_∞ controller